

SUPPORTING INFORMATION

In-situ formation of cellular graphene framework in thermoplastic composites leading to superior thermal conductivity

Fakhr E. Alam ^{a,b,1}, Wen Dai ^{a,b,1}, Minghui Yang ^c, Shiyu Du ^d, Xinming Li ^e, Jinhong Yu ^{a*}, Nan Jiang ^{a*}, Cheng-Te Lin ^{a,b*}

^a *Key Laboratory of Marine Materials and Related Technologies, Zhejiang Key Laboratory of Marine Materials and Protective Technologies, Ningbo Institute of Materials Technology and Engineering (NIMTE), Chinese Academy of Sciences, Ningbo 315201, China. *E-mail: yujinhong@nimte.ac.cn (J.H Yu); jiangnan@nimte.ac.cn (N. Jiang); linzhengde@nimte.ac.cn (C.-T. Lin)*

^b *University of Chinese Academy of Sciences, 19 A Yuquan Rd., Shijingshan District, Beijing 100049, China.*

^c *Ningbo Institute of Materials Technology and Engineering (NIMTE), Chinese Academy of Sciences, Ningbo 315201, China.*

^d *Division of Functional Materials and Nanodevices, Ningbo Institute of Materials Technology and Engineering, Chinese Academy of Sciences, Ningbo, Zhejiang 315201, China.*

^e *Department of Electronic Engineering, The Chinese University of Hong Kong, Hong Kong SAR, China.*

¹ *Fakhr E Alam and Wen Dai Contributed equally to this work.*

SUPPLEMENT

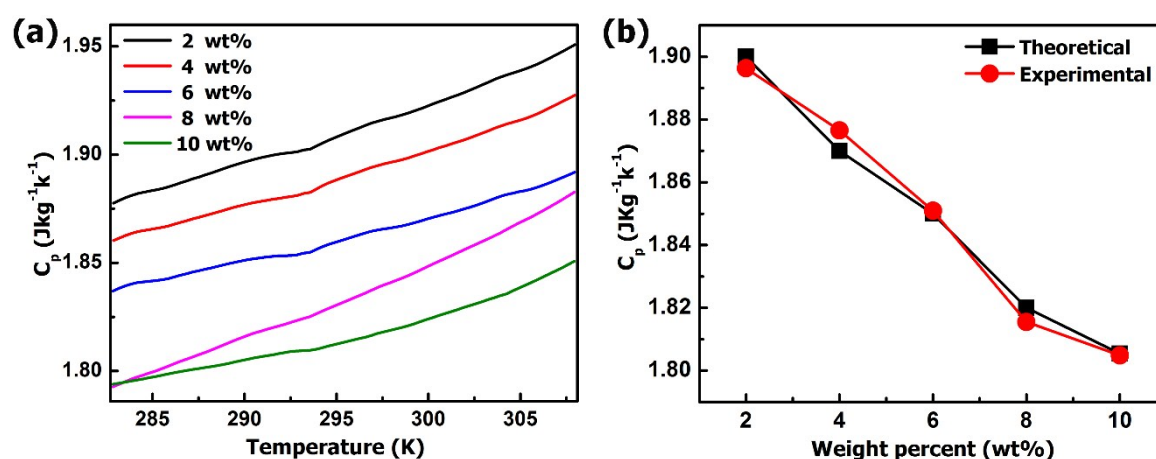


Fig. S1. Specific heat capacity (C_p) of GNP/PP composites with various GNP loadings at temperature range of 282 – 308 K. (b) The comparison between theoretical and experimental C_p of GNP/PP composites at room temperature.

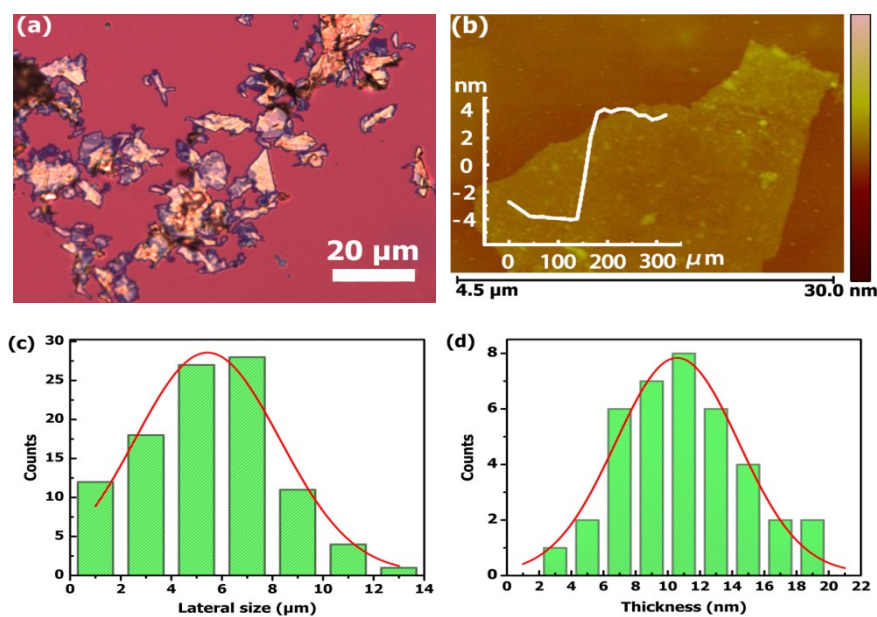


Fig. S2. The characterization of GNPs: (a) OM and (b) AFM images; the distribution of (c) lateral size and (d) thickness.

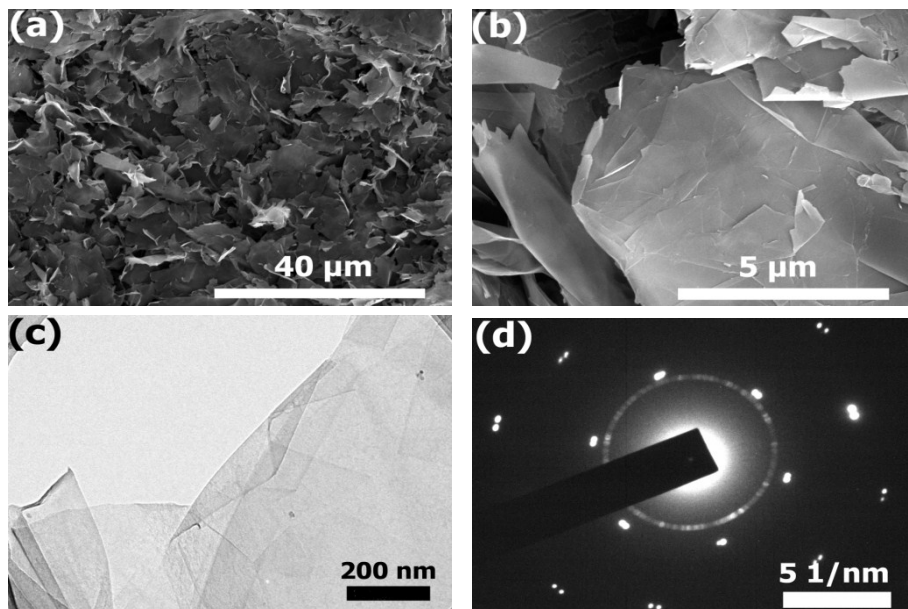


Fig. S3. (a) Low and (b) High-magnification SEM images of GNPs. (c) TEM image of an individual GNP and (d) Selected area diffraction pattern of (c).

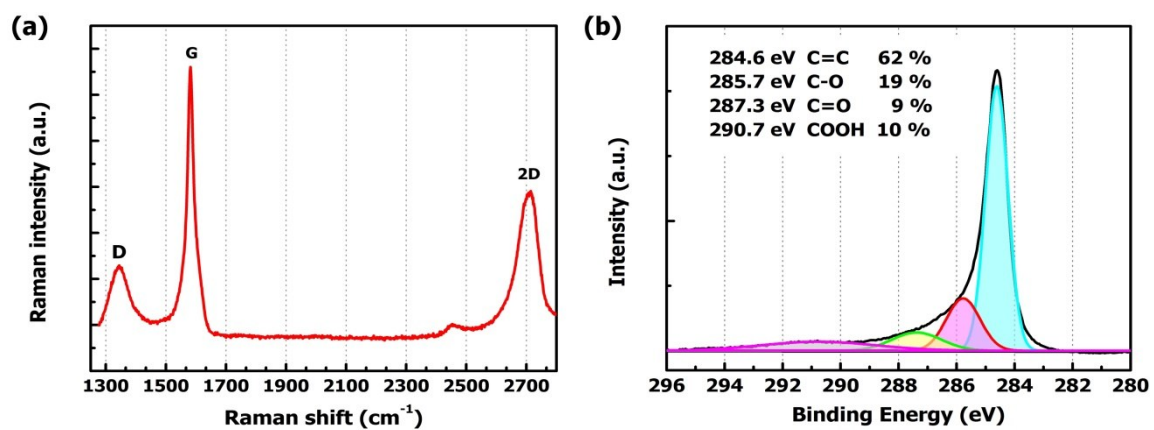


Fig. S4. (a) Raman and (b) XPS C1s spectra of GNPs.

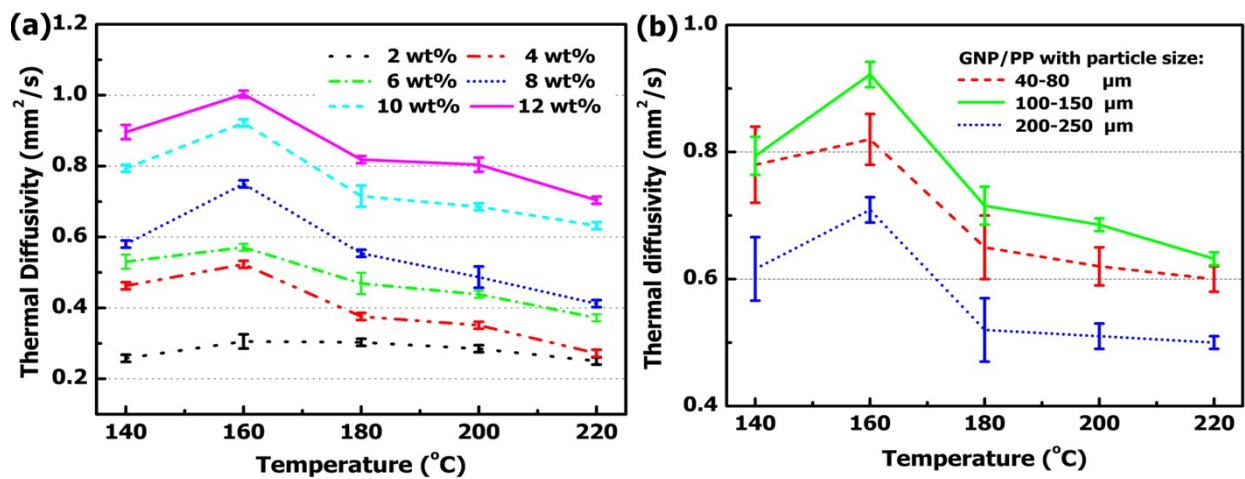


Fig. S5. Thermal diffusivity of GNP/PP composites (a) prepared at various GNP loadings and hot-pressing temperatures and (b) made with different PP particle sizes.

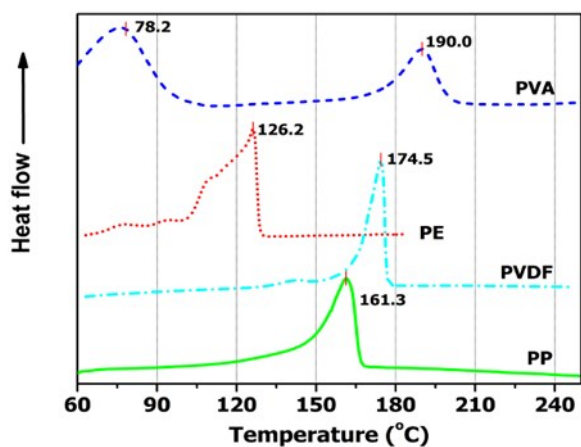


Fig. S6. DSC curves of neat thermoplastic polymers used in this study.

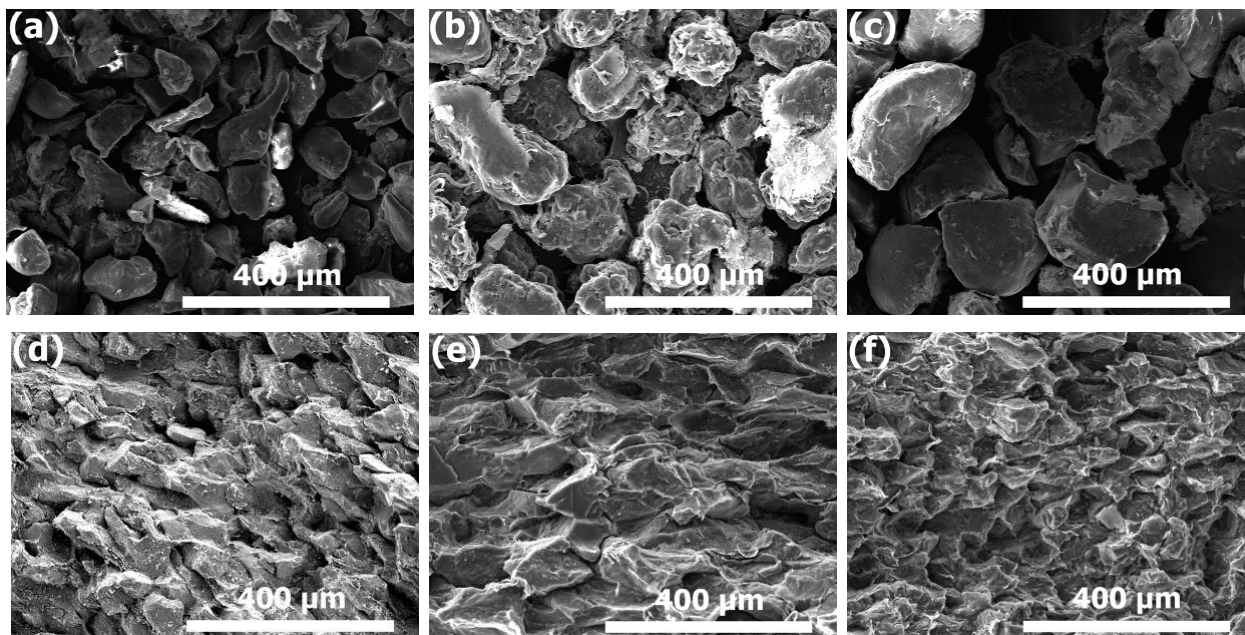


Fig. S7. SEM images of GNP-coated PP particles with the size of (a) 40 – 80; (b) 100 – 150; (c) 200 – 250 μm and the section view of hot-pressed PP composites made using (d) 40 – 80; (e) 100 – 150; (f) 200 – 250 μm sized PP.

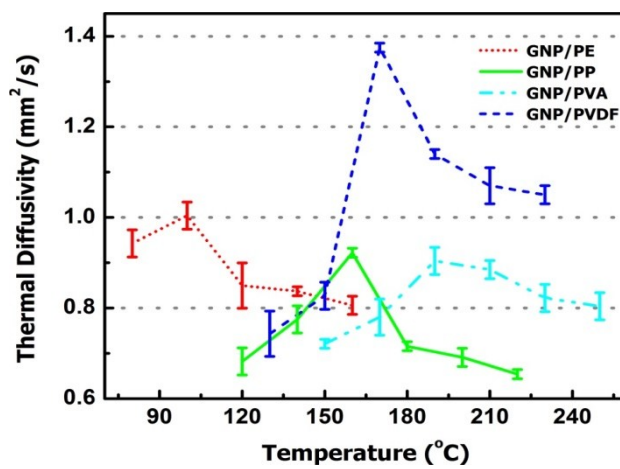


Fig. S8. Thermal diffusivity of the thermoplastic composites with 10 wt% GNP loading as a function of the pressing temperatures.

Table S1. A comparison of the thermal conductivity and TCE of thermoplastic composites made with graphene and white graphene (boron nitride, BN).

Filler	Matrix	Content (wt%)	Thermal Conductivity ($\text{Wm}^{-1}\text{K}^{-1}$)	TCE (%)	Reference
BN	PE	50	1.38	319	1
BN Nanosheets	PE	50	1.19	260	1
GNPs	PE	10	1.84	457	Our work
Expanded Graphite	PVDF	15	0.9	373	2
Graphite Nanosheets	PVDF	15	1.28	573	2
BN	PVDF	20	0.97	322	3
GNPs	PVDF	10	1.47	673	Our work
BN	PVA	10	0.44	109	4
GNPs	PVA	10	1.43	580	Our work

References

1. P. G. Ren, X. H. Si, Z. F. Sun, F. Ren, L. Pei and S. Y. Hou, *J. Polym. Res.*, 2016, **23**, 1-11.
2. S. Deng, Y. Zhu, X. Qi, W. Yu, F. Chen and Q. Fu, *RSC Adv.*, 2016, **6**, 45578-45584.
3. Y. J. Xiao, W. Y. Wang, T. Lin, X. J. Chen, Y. T. Zhang, J. H. Yang, Y. Wang and Z. W. Zhou, *J. Phys. Chem. C*, 2016, **120**, 6344-6355.
4. B.-H. Xie, X. Huang and G.-J. Zhang, *Compos. Sci. Technol.*, 2013, **85**, 98-103.